Partially Wetted Catalyst Performance in the Consecutive-Parallel Network

In this study the impact of the transport processes and the degree of wetting on the overall selectivity of a single catalytic pellet is examined for the commercially important consecutive-parallel network $A_{(g)} + \nu_B B_{(l)} \rightarrow \nu_{R1} R_{(l)}$, $A_{(g)} + \nu_{R2} R_{(l)} \rightarrow P_{(l)}$. The one-dimensional formulation applies to catalysts in which the active component is concentrated in a thin porous surface shell coating an impermeable support. Model modifications provide an approximate description of uniformly active catalysts. The kinetics are assumed to be first and zero order with respect to the volatile (A) and nonvolatile (B, R) components, respectively, as encountered in many olefin hydrogenations. The common literature assumption of volatile reactant limiting reactions is relaxed by accounting for nonvolatile reactant depletion. The depletion can significantly reduce the desired product (R) selectivity below its intrinsic value attained under fully wetted, no-depletion conditions. A model employing the single limiting reactant assumption cannot predict such selectivity variations. The selectivity is shown to be a complex function of the wetting efficiency, the stoichiometry, and the interacting reactions and mass transport processes. In many cases the intrinsic selectivity is attained for wetting efficiencies exceeding a critical value. Increases in the wetting above this value can reduce significantly the production rate of R because of resistance to A supply through the liquid film. Thus, an optimal range of wetting efficiencies exists for which the selectivity is equal to its intrinsic value and overall rates are high. The significance of the main findings with regard to trickle-bed reactor performance are discussed.

Michael P. Harold
Department of Chemical Engineering
University of Massachusetts
Amherst, MA 01003

Introduction

Many commercially important chemicals are one of several products in a complex chemically reacting system. It is crucial for reactor design to determine how mass transport processes, heat effects, and mixing interact with the intrinsic kinetics to alter the product distributions. Pioneering studies of gas-liquid multireaction systems were presented by van de Vusse (1966a,b), Hashimoto et al. (1968), Teramoto et al. (1969), and Ding et al. (1974), and studies of single-phase heterogeneous catalytic multireaction systems were presented by Wheeler (1955), Wei (1962), Butt (1966), and Roberts (1972).

The cocurrent downflow trickle-bed reactor is commonly employed to carry out catalytic reactions between volatile and nonvolatile components. Depending on the relative gas and liquid flow rates and packing characteristics, several flow regimes are possible (Sato et al., 1973; Satterfield, 1975; Gianetto et al., 1978). Most common in practice is trickling flow, which involves film and rivulet flow over the catalyst with the flowing gas occupying the remaining void space. Because of nonuniform packing features, improper liquid feed distribution, or the use of low gas and liquid rates, a fraction of the external surface of the catalyst pellets may not be wetted. In fact, each pellet may be exposed to a unique wetting environment consisting of films, rivulets, pendular structures, and liquid pockets (Ng, 1986). The catalyst void typically is filled with liquid because of strong capillary forces for reactions without significant exothermicity or volatile reaction products (Schwartz et al., 1976). The effect

of this incomplete (partial) wetting on the reactor performance is a distinguishing, complicating feature of the trickle-bed reactor.

A number of studies have appeared that considered partial external wetting effects on catalyst performance in single reaction systems (Ramachandran and Smith, 1979; Mills and Dudukovic, 1979; Herskowitz et al., 1979; Tan and Smith, 1980; Goto et al., 1981; Herskowitz, 1981a; Sakornwimon and Sylvester, 1982; Ring and Missen, 1986; Gabitto et al., 1986; Dassori et al., 1987; Yentekakis and Vayenas, 1987; Beaudry et al., 1987; Harold and Ng, 1987; among others). These studies have shown that partial wetting can enhance or retard the overall rate depending on which process is rate controlling and which reactant is limiting. A limitation of most of the earlier studies is the assumption that one reactant is in excess throughout the entire pellet. Harold and Ng (1987) and Beaudry et al. (1987) demonstrated the significant impact of liquid reactant depletion on the effectiveness for a supposedly gas reactant limited reaction.

To the contrary, only a few studies have addressed the features of multireaction gas-liquid catalytic systems for which partial wetting of the catalyst pellets occurs. This is despite the large number of commercial reaction systems that fall into this category. Examples include hydrodesulfurization and hydrodenitrogenation (Gates et al., 1979), hydrogenation of acetylenic and diolefinic compounds (White and Litt, 1975; Somers et al., 1976; Kawakami and Kusunoki, 1976), the ethynylation of formaldehyde to butynediol (Kale et al., 1981), and many others. Herskowitz (1981b) showed for the unimolecular consecutive reaction network ($A \rightarrow R \rightarrow P$) that the selectivity of R attains a maximum value at an intermediate wetting efficiency under certain conditions. Stegmuller et al. (1986) demonstrated that the selectivity of the intermediate in the consecutive-parallel network is maximized at an intermediate external mass transfer rate of the limiting reactant for certain combinations of reaction orders. Similar conclusions were reached by Gabitto et al. (1986) for a parallel network. In these studies, however, the issue of a finite supply of the "excess" nonvolatile reactants was not addressed.

Many experimental studies have appeared involving multiple catalytic hydrogenation reactions in slurry reactors (Kawakami et al., 1976; Marangozis et al., 1977; Wisniak and Simon, 1979), trickle-bed reactors (Mochizuki and Matsui, 1976; Somers et al., 1976; Satterfield and Yang, 1984; Kohler and Richarz, 1986; Rueker et al., 1987), and other reactor types (Kawakami and Kusunoki, 1976; White and Litt, 1975). These studies demonstrate the complex influence of external and intraparticle diffusion limitations on the product distributions. Since partial external wetting significantly influences the mass transport processes, it is likely that the product distributions will also be affected. Kohler and Richarz (1986) observed significant product distribution changes during the complex reaction of aniline, acetone, and hydrogen over a palladium catalyst. They observed that the catalyst was not completely wetted although they did not indicate its effect on the selectivity variations. Rueker et al. (1987) observed a significant effect of liquid to catalyst contacting efficiency on the overall conversion of biphenyl to the intermediate cyclohexylbenzene and the final product bicyclohexane. However, they did not indicate how the degree of wetting may improve the desired product selectivity.

A better understanding is needed of the impact of partial wetting on trickle-bed reactor performance for multireaction systems. The objective of this work is to investigate the direct relationship between selectivity and wetting efficiency of a single catalytic pellet in which a consecutive-parallel liquid phase catalytic reaction network occurs:

$$\text{Reaction 1: } A_{(g)} + \nu_B B_{(l)} \rightarrow \nu_{R1} R_{(l)}$$

$$\text{Reaction 2: } A_{(g)} + \nu_{R2} R_{(l)} \rightarrow P_{(l)}$$

The volatile (g) species A reacts in a parallel fashion and nonvolatile (l) R reacts consecutively. This network is representative of many commercial systems, some of which are listed in Table 1.

The multireaction partially wetted pellet model developed in this study is based on the one-dimensional formulation of Harold and Ng (1987) for the single reaction system. The rates of each reaction are assumed to be first order in A and zero order in B and R; i.e.,

$$r_1 = k_1 C_A H(C_B) \tag{1a}$$

$$r_2 = k_2 C_A H(C_R) \tag{1b}$$

where H is the Heaviside function. By accounting for nonvolatile reactant depletion, the common literature assumption of the single limiting (volatile) reactant is relaxed. The model is formally valid for a surface shell impregnated, washcoated cata-

Table 1. Some Gas-Liquid Catalytic Reaction Systems with the Consecutive-Parallel Network Form: $A + B \rightarrow R, A + R \rightarrow P$

No.	Volatile Reactant, A	Nonvolatile Reactant, B	Intermed. Product, R	Final Product, P	Catalyst	Ref.
1	Hydrogen	Phenylacetylene	Styrene	Ethylbenzene	Pt/Al_2O_3 Pd film	Kawakami & Kusunoki (1976) White & Litt (1975)
2	Hydrogen	Biphenyl	Cyclohexylbenzene	Bicyclohexane	$NiO\text{-}MoO_3/Al_2O_3$	Ruecker et al. (1987)
3	Hydrogen	Diolefinic compound	Mono-olefin	Saturated hydrocarbon	Gulf catalyst	Somers et al. (1976)
4	Hydrogen	Linoleic acid	Cis- and trans-oleic acid	Saturated oil	Nickel	Marangozis et al. (1977)
5	Hydrogen	Dibenzothiophene	Biphenyl[1]	Cyclohexylbenzene[1]	$CoO\text{-}MoO_3/Al_2O_3$	Broderick & Gates (1981)
6	Acetylene[2]	Formaldehyde	Propargyl alcohol	Butynediol	Copper acetylide/ silica gel	Kale et al. (1981)
7	Hydrogen[2]	Aniline + Acetone → Schiffbase (B)	Isopropylaniline	Phenylcyclohexylamine	Pt/Al_2O_3	Kohler & Richarz (1986)

[1]Hydrogenolysis products; parallel hydrogenation pathway possible
[2]Other side reactions possible

lyst, although an approximate method is developed to model the uniformly active pellet. It is shown that a reduction in the desired product selectivity results from depletion of the nonvolatile reactants, which is a direct consequence of the partial wetting and mass transport limitations. The model is used to simulate the performance of a partially wetted catalyst in which rapid, mass transport limited reactions occur. A prototype system is the palladium on alumina catalyzed phenylacetylene hydrogenation to the intermediate styrene and the final product ethylbenzene. Previous kinetics studies show that both reactions are fast and are first order in the hydrogen and zero order in the nonvolatile reactants (White and Litt, 1975, and references therein).

Although the modeled single pellet is admittedly idealized with regard to the geometry and reaction kinetics, key qualitative trends are identified without resorting to more complex models and numerical integrations. At this stage, the main utility of the model is in preliminary trickle-bed reactor design. The simulations help to elucidate the interplay between the partial wetting, several transport processes, and nonvolatile reactant depletion. To this end, the wetting efficiencies required to maximize the desired product yield are determined.

The Physical Picture

The catalytic pellet is assumed to have the active component concentrated in a thin surface shell of thickness Δ (y direction, Figure 1). The pellet half-width is $S/2$ (x direction) and length is L (z direction). This geometry applies to washcoated catalysts in which an impermeable core is covered with a porous layer impregnated with the active component. The active shell is sufficiently thin that curvature effects can be ignored. To a first approximation, the model can be applied to completely porous surface shell catalysts, or to uniformly impregnated, arbitrarily shaped catalysts with an active volume $V_{p,act}$ and external area S_x. In the latter cases Δ is the characteristic diffusion length $V_{p,act}/S_x$. In all cases the pellet width S is equal to the perimeter of the surface available for wetting. A fraction (E_w, the wetting efficiency) of the external surface is wetted by a liquid film of uniform thickness and width in the direction of flow. Only half of the active zone needs to be considered since lines of symmetry exist at the center of the wetted ($x = 0$) and nonwetted ($x = S/2$) parts. The pellet pore volume is assumed to be filled with liquid. The liquid contains a mixture of the nonvolatile species B, R, and P, the dissolved volatile reactant A, and possibly an inert, nonvolatile solvent. From this point, species R is considered the desired product.

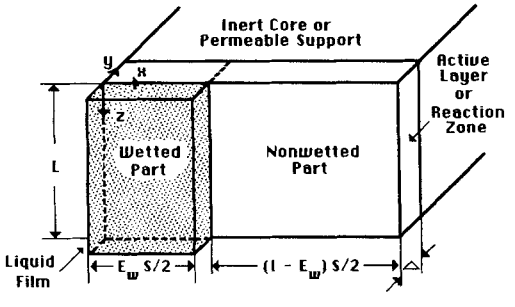

Figure 1. Half of a partially wetted pellet.

The pair of isothermal, irreversible liquid-phase catalytic reactions identified above occur within the pellet. Justification for the zero-order dependence on the nonvolatile reactants B and R, Eqs. 1a–1b, is that they are in large excess. As mentioned earlier, these kinetics are followed by some hydrogenation reactions. An attractive feature of this rate model is that closed-form solutions can be obtained. This enables an efficient examination of the interplay between the partial wetting and the mass transport and reaction processes. In the more general cases the rates will depend on the nonvolatile reactant concentrations if B and R are not in excess everywhere within the pellet. The use of such other bimolecular kinetic rate expressions requires nontrivial numerical integrations. A comparison of the predictions of the one-dimensional single reaction model, which assumes a zero-order nonvolatile reactant dependence, to the two-dimensional model, which assumes a first-order dependence, reveals very good qualitative agreement (Harold and Ng, 1987; Funk et al., 1988). Thus, it is expected that the qualitative trends are similar to the model with kinetics that are first order with respect to species B and R.

Several transport processes occur at the single pellet level. The volatile reactant A enters the pellet from the liquid film or from the gas. The nonvolatile liquid reactant B can enter only from the liquid film. Species R either enters or leaves the pellet via the liquid film, i.e., there is either a net consumption or formation of R. Intraparticle mass transport from front to back ($y = 0$ to Δ) and laterally ($x = 0$ to $S/2$) is by diffusion, which occurs in parallel with the reactions. If the aspect ratio of the pellet [$\alpha = (S/2)/\Delta$] is sufficiently large and/or the catalytic activity is sufficiently small, such that the criteria

$$\Delta\sqrt{\frac{k_1}{D_{Ae}}} < 0.1, \quad \Delta\sqrt{\frac{k_2}{D_{Ae}}} < 0.1 \tag{2}$$

are both satisfied, then intraparticle gradients in the direction (y) normal to the wetted surface are insignificant. In this case we can safely assume uniform intraparticle concentrations in the y direction. If either criterion is violated there will be nonnegligible concentration gradients in the y direction for species A, and possibly for B and R. In this event, the scheme developed by Harold and Ng (1987) for the single reaction system to approximate the y-directed intraparticle diffusion and reaction process is applied.

Model Development

Differential mass balances

For the moment we assume an infinite supply rate of the liquid reactants B and R and ignore possible intraparticle gradients in the y direction. In the wetted (w) part of the pellet [$0 < s = x/(S/2) < E_w$] species A, B, and R respectively satisfy

$$\frac{d^2u_{A,w}}{ds^2} + \alpha Bi_{A,w}(1 - u_{A,w}) - [\phi^2 u_{A,w} H(u_{B,w}) + \delta\phi^2 u_{A,w} H(u_{R,w})] = 0 \tag{3}$$

$$\frac{d^2u_{B,w}}{ds^2} + \alpha Bi_{B,w}(u_{Bf} - u_{B,w}) - m_B\phi^2 u_{A,w} H(u_{B,w}) = 0 \tag{4}$$

$$\frac{d^2u_{R,w}}{ds^2} + \alpha Bi_{R,w}(u_{Rf} - u_{R,w}) - [m_{R2}\delta\phi^2 u_{A,w}H(u_{R,w}) - m_{R1}\phi^2 u_{A,w}H(u_{B,w})] = 0 \quad (5)$$

In the nonwetted (n) part ($E_w < s < 1$) species A, B, and R respectively satisfy

$$\frac{d^2u_{A,n}}{ds^2} + \alpha Bi_{A,n}(1 - u_{A,n}) - [\phi^2 u_{A,n}H(u_{B,n}) + \delta\phi^2 u_{A,n}H(u_{R,n})] = 0 \quad (6)$$

$$\frac{d^2u_{B,n}}{ds^2} - m_B\phi^2 u_{A,n}H(u_{B,n}) = 0 \quad (7)$$

$$\frac{d^2u_{R,n}}{ds^2} - [m_{R2}\delta\phi^2 u_{A,n}H(u_{R,n}) - m_{R1}\phi^2 u_{A,n}H(u_{B,n})] = 0 \quad (8)$$

The dimensionless variables and parameters are defined as

$$u_{A,j} = \frac{C_{A,j}}{C_{Ae}} \quad u_{B,j} = \frac{C_{B,j}}{C_{Ae}} \quad u_{R,j} = \frac{C_{R,j}}{C_{Ae}} \quad (j \equiv w, n)$$

$$s = \frac{x}{S/2} \quad Bi_{A,w} = \frac{Sk_{A,w}}{2D_{Ae}} \quad Bi_{A,n} = \frac{Sk_{A,n}}{2D_{Ae}}$$

$$Bi_B = \frac{Sk_B}{2D_{Be}} \quad Bi_R = \frac{Sk_R}{2D_{Re}} \quad \phi^2 = \left(\frac{S}{2}\right)^2 \frac{k_1}{D_{Ae}} \quad \delta = \frac{k_2}{k_1}$$

$$u_{Bf} = \frac{C_{Bf}}{C_{Ae}} \quad u_{Rf} = \frac{C_{Rf}}{C_{Ae}} \quad \alpha = \frac{S/2}{\Delta} \quad m_B = \frac{\nu_B D_{Ae}}{D_{Be}}$$

$$m_R = \frac{(\delta\nu_{R2} - \nu_{R1})D_{Ae}}{D_{Re}} = \delta m_{R2} - m_{R1} \quad (9)$$

The model has 13 parameters (E_w, δ, ϕ, α, $Bi_{A,w}$, $Bi_{A,n}$, Bi_B, Bi_R, u_{Bf}, u_{Rf}, m_B, m_{R1}, m_{R2}).

Equations 3–8 describe the interacting processes of intraparticle diffusion in the x (i.e., s) direction, the chemical reaction(s), and transport between the catalyst and the surroundings in the direction (y) normal to the wetted surface. Species A is consumed by both reactions and is supplied from the liquid film on the wetted part and directly from the gas on the nonwetted part. C_{Ae} is the species A equilibrium liquid phase concentration for its given partial pressure in the surrounding gas. Nonvolatile species B is consumed by reaction 1 and is only supplied from the liquid film, within which its average concentration is C_{Bf}. Nonvolatile species R is consumed by reaction 2 and produced by reaction 1 and has an average liquid film concentration C_{Rf}. The liquid film either supplies or removes R depending on the value of C_{Rf} relative to the intraparticle concentration C_R at a fixed lateral (s) position.

Nonvolatile species depletion: Identification of possible cases

If species B is not supplied at an infinite rate then both B and R may deplete within the pellet. This is the distinguishing feature of the coupling of a zero-order reaction and mass transport (Lin and Lih, 1971; Roberts, 1972; Aris, 1975; Harold and Ng, 1987). Depletion is possible if the species B external supply rate and/or the intraparticle diffusion process is slower than its consumption rate by reaction. Since nonvolatile B and R are only supplied from the liquid film, a reduced wetting efficiency makes depletion even more likely. For the completely nonwetted pellet at steady state, B and R deplete completely since the reactions are irreversible.

Figure 2 shows the ten possible cases for this reaction system. Each X denotes a point of depletion. Each case corresponds to a different positioning of the point of B depletion (s_B^*) and the point of R depletion (s_R^*) relative to the center of the wetted zone ($s = 0$), the wetted-nonwetted boundary ($s = E_w$), and the center of the nonwetted zone ($s = 1$). s_B^* and s_R^* must be computed if either or both is between $s = 0$ and 1 (cases 2–9). For some of the cases one or both of the nonvolatile reactants do not deplete or deplete completely; these cases are depicted by $s_i^* > 1$ ($i = A$ and/or B) and $s_i^* < 0$, respectively. For each case there are two or more regions formed by $s = 0$, E_w, 1, and the depletion points s_B^* and s_R^*.

For each case, A, B, and R satisfy appropriate differential mass balances within each region, as summarized in Table 2 and now described. Suppose the pellet is almost fully wetted ($E_w \to 1$) and the reactions are sufficiently slow compared to the mass transport processes so that B and R do not deplete ($s_B^* > 1, s_R^* > 1$). For this case 1, there is a nonwetted and wetted region. The governing mass balances for A, B, and R are identical to Eqs. 3–8 with subscripts 1(2) replacing $w(d)$. For a sufficient increase in the catalytic activity (k_1, k_2) the species B external supply rate and/or intraparticle diffusion may not be rapid enough to supply B to points well into the zone beneath the nonwetted surface. This case 2 corresponds to B depletion in the nonwetted zone without R depletion ($E_w < s_B^* < 1, s_R^* > 1$). In

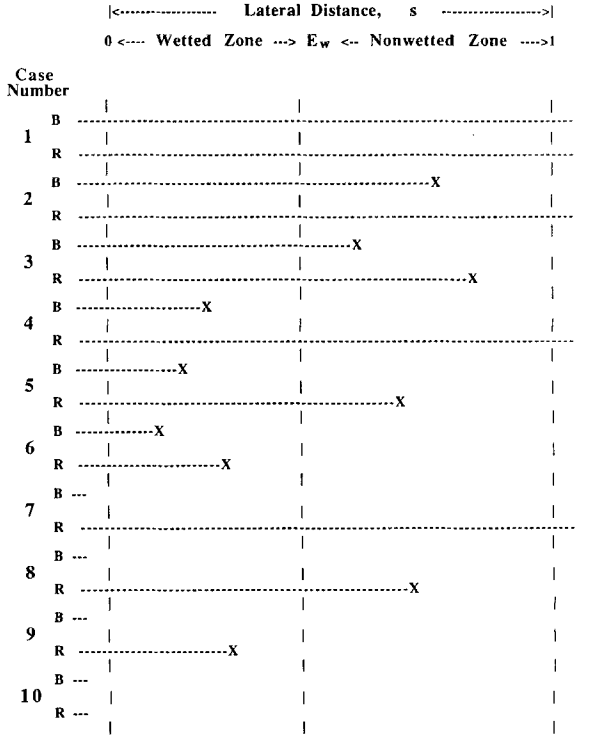

Figure 2. Classification of the ten cases corresponding to possible relative locations of points of *B* and *R* depletion.

Table 2. Summary of Governing Species A, B, and R Differential Mass Balances for the Ten Cases

Wetted Zone ($0 < s < E_w$)

Species

A: $\dfrac{d^2u_{Ai}}{ds^2} + \alpha Bi_{A1}(1 - u_{Ai}) - r_{A,w} = 0$

B: $\dfrac{d^2u_{Bi}}{ds^2} + \alpha Bi_B(u_{Bf} - u_{Bi}) - r_{B,w} = 0$

R: $\dfrac{d^2u_{Ri}}{ds^2} + \alpha Bi_R(u_{Rf} - u_{Ri}) - r_{R,w} = 0$

	Reaction Terms	Cases	Region No., i
$r_{A,w}$:	$(1 + \delta)\phi^2u_{Ai}$	1–6	1
	$\delta\phi^2u_{Ai} + \dfrac{\alpha Bi_Bu_{Bf}}{m_B}$	4–6	2
		7–9	1
	$\dfrac{\alpha Bi_Bu_{Bf}}{m_B} + \dfrac{\alpha Bi_Ru_{Rf}}{m_{R2}} + \dfrac{\alpha Bi_Bu_{Bf}m_{R1}}{m_Bm_{R2}}$	6	3
		9	2
		10	1
$r_{B,w}$:	$m_B\phi^2u_{Ai}$	1–6	1
	0	4–6, 9	2
		6	3
		7–10	1
$r_{R,w}$:	$m_R\phi^2u_{Ai}$	1–6	1
	$m_{R2}\delta\phi^2u_{Ai} - \dfrac{\alpha Bi_Bu_{Bf}m_{R1}}{m_B}$	4–6	2
		7–9	1
	0	6	3
		9	2
		10	1

Table 2. (Continued)

Nonwetted Zone ($E_w < s < 1$)

Species

A: $\dfrac{d^2u_{Ai}}{ds^2} + \alpha Bi_{A2}(1 - u_{Ai}) - r_{A,n} = 0$

B: $\dfrac{d^2u_{Bi}}{ds^2} - r_{B,n} = 0$

R: $\dfrac{d^2u_{Ri}}{ds^2} - r_{R,n} = 0$

	Reaction Terms	Cases	Region No., i
$r_{A,n}$:	$(1 + \delta)\phi^2u_{Ai}$	1–3	2
	$\delta\phi^2u_{Ai}$	2–5	3
		7, 8	2
	0	3, 5, 6	4
		8, 9	3
		10	2
$r_{B,n}$:	$m_B\phi^2u_{Ai}$	1–3	2
	0	2–5, 8, 9	3
		3, 5, 6	4
		7, 8, 10	2
$r_{R,n}$:	$m_R\phi^2u_{Ai}$	1–3	2
	$m_{R2}\delta\phi^2u_{Ai}$	2–5	3
		7, 8	2
	0	3, 5, 6	4
		8, 9	3
		10	2

addition to the two regions encountered for case 1, a third region appears in which B is depleted and only reaction 2 occurs. In this region 3, A is consumed at a rate equal to $\delta\phi^2u_{A3}$; the rate of R consumption is $m_{R2}\delta\phi^2u_{A3}$. If the formation and supply rate of R is not sufficiently fast R may also deplete at some point s_R^* between s_B^* and 1. This is case 3 ($E_w < s_B^* < s_R^* < 1$). A fourth region is created within which both B and R are depleted and into which A enters from the gas and diffuses but does not react. Note that as long as there is some B present, reaction 1 proceeds, thus preventing depletion of R; i.e., $s_R^* > s_B^*$ necessarily.

Additional increases in the activity and/or reductions in the B and R supply rates can result in depletion of both B and R within the wetted zone (cases 4–10). Cases 4–6 correspond to B depletion in the wetted zone without any R depletion (case 4: $0 < s_B^* < E_w$, $s_R^* > 1$), with R depletion in the nonwetted zone (case 5: $0 < s_B^* < E_w < s_R^* < 1$), and with R depletion between the B depletion point and the wetted-nonwetted boundary (case 6: $0 < s_B^* < s_R^* < E_w$).

In cases 4–6 the supply rate of B is sufficiently slow that it is completely consumed in part of the wetted zone (region 2). In the adjacent region 1 both B and R are present and the governing equations are identical to those for region 1 in cases 1–3. In region 2, the total rate of A consumption is $\delta\phi^2u_{A2} + \alpha Bi_Bu_{Bf}/m_B$. The first(second) term is the consumption rate by reaction 2(1). The second term denotes that the reaction 1 rate is controlled by the species B supply rate, k_BC_{Bf}/Δ. Thus, the net consumption rate of R is $m_{R2}\delta\phi^2u_{A2} - \alpha Bi_Bu_{Bf}m_{R1}/m_B$. For cases 4 and 5, region 3 corresponds to a nonwetted zone in which reaction 2 proceeds. For case 5(6) R depletes within the nonwetted(wetted) zone. Depletion of R in the wetted zone (region 3 of case 6) occurs if the combined R supply rate from the liquid film and production rate by the B supply rate limited reaction 1 is slower than the R consumption rate by reaction 2. In this region the total A consumption rate is $\alpha Bi_Bu_{Bf}/m_B + \alpha Bi_Ru_{Rf}/m_{R2} + \alpha Bi_Bu_{Bf}m_{R1}/m_{R2}m_B$. The first term is the consumption rate by reaction 1. The second and third terms, the dimensionless forms of $(k_RC_{Rf}/\Delta)/\nu_{R2}$ and $(k_BC_{Bf}/\Delta)(\nu_{R1}/\nu_B\nu_{R2})$, represent the A consumption rate by reaction 2, which is the sum of the supply rate of R (second term) and the production rate of R by the B supply rate limited reaction 1 (third term). For cases 5 and 6 there is a nonwetted region 4 in which neither reaction occurs.

Cases 7–10 correspond to complete B depletion ($s_B^* < 0$) with no R depletion (case 7: $s_R^* > 1$), R depletion in the nonwetted zone (case 8: $E_w < s_R^* < 1$), R depletion in the wetted zone (case 9: $0 < s_R^* < E_w$), and complete R depletion (case 10: $s_R^* < 0$). The equations are similar to cases 4–6.

Boundary conditions and model solutions

Analytical general solutions for the A, B, and R concentration profiles are in the form of hyperbolic functions. These are pro-

vided in Supplementary Material B for the ten cases. Solution for the integration constants requires boundary conditions that are now described (summarized in Table 3). At the center of the wetted zone ($s = 0$) the no-flux condition applies for each species because of symmetry. The same holds true for the center of the nonwetted zone ($s = 1$). For cases 1 (no depletion), 7 (complete B and no R depletion), and 10 (complete B and R depletion) the remaining conditions are concentration and flux continuity at the wetted-nonwetted boundary ($s = E_w$). After some manipulations, expressions for the integration constants are obtained. These are provided in Supplementary Material C. For the remaining cases 2–6, 8, and 9, concentration and flux continuity also apply at $s = s_B^*$ (if applicable), and $s = s_R^*$ (if applicable). Depletion and continuity demands that $u_B(s_B^*) = du_B/ds(s_B^*) = 0$ and $u_R(s_R^*) = du_R/ds(s_R^*) = 0$. The vanishing B and R concentration conditions are the additional ones necessary to compute s_B^* and s_R^*. After some cumbersome algebraic manipulations, expressions for the integration constants and either one or two implicit functions of s_B^* and s_R^* ($F_{j,k} = 0; j = 2, \ldots, 6, 8, 9$; $k = 1$ or 2) are derived. These are provided in Supplementary Material C. For cases 2 and 4 (8 and 9) a single function that implicitly contains s_B^* (s_R^*) is obtained. For cases 3, 5, and 6 two functions that implicitly contain s_B^* and s_R^* are obtained.

Table 3. Governing Boundary Conditions for the Ten Cases

Cases 1–10
No flux at lines of symmetry
$\frac{du_i}{ds} = 0 \quad \text{at } s = 0, 1; \quad i \equiv A, B, R$
Continuity of concentration and flux at wetted-nonwetted boundary
$u_{ik} = u_{ik+1}$
$\frac{du_{ik}}{ds} = \frac{du_{ik+1}}{ds} \quad \text{at } s = E_w;$
$i \equiv A, B, R; \quad k \equiv$ region number (1, 2, or 3)
Cases 2–6
Depletion of B condition
$u_B = 0 \quad \text{at } s = s_B^*$
Continuity of concentration and flux at B depletion point
$u_{ik} = u_{ik+1}$
$\frac{du_{ik}}{ds} = \frac{du_{ik+1}}{ds} \quad \text{at } s = s_B^*;$
$i \equiv A, B, R; \quad k \equiv$ region number (1, 2, or 3)
Cases 3, 5, 6, 8, 9
Depletion of R condition
$u_R = 0 \quad \text{at } s = s_R^*$
Continuity of concentration and flux at R depletion point
$u_{ik} = u_{ik+1}$
$\frac{du_{ik}}{ds} = \frac{du_{ik+1}}{ds} \quad \text{at } s = s_R^*;$
$i \equiv A, B, R; \quad k \equiv$ region number (1, 2, or 3)

Modification to account for diffusional resistance in the y direction

In order to model reaction systems that do not satisfy the criteria in Eq. 2 the contribution of intraparticle gradients in the direction (y) normal to the wetted surface must be included. The approach is to modify the overall transport coefficients $k_{A,n}$, $k_{A,w}$, k_B, and k_R and retain the same governing equations. Details of the analysis are given in Supplementary Material A; here they are briefly highlighted.

The overall resistance to species i transport in the y direction at any x position is the reciprocal of the transport coefficient for that species, k_i ($i = A, B, R$). This resistance is assumed to be a sum of an external resistance and an intraparticle resistance component:

$$\frac{1}{k_i} = \frac{1}{k_i^o} + \frac{\Delta_i^*}{D_{ie}} \tag{10}$$

Δ_i^* is an effective diffusion length for species i which contains the contribution of the intraparticle diffusion and reaction. The ratio D_{ie}/Δ_i^* is an effective transport coefficient. At steady state, the external transport flux is equal to an approximate expression for the intraparticle transport flux:

$$k_i^o[C_{if} - (C_{iy})_s] = \frac{D_{ie}}{\Delta_i^*}[(C_{iy})_s - \hat{C}_{iy}] \tag{11}$$

The subscript y on the concentration terms denotes that gradients in the x direction are not accounted for in this analysis. $(C_{iy})_s$ and (C_{if}) are the surface and bulk concentrations of species i (noting that $C_{Af} = C_{Ae}$) and $\hat{C}_{iy}$ is the average concentration over $y \in [0, \Delta]$. $\hat{C}_{iy}$ is determined from the solution to one-dimensional (y) diffusion and reaction in a catalytic slab of half-thickness Δ. This result is substituted into Eq. 11 and the result is compared to the exact expression for the surface flux. This gives an expression for Δ_i^*, which is then substituted into Eq. 10.

The results are as follows. The overall mass transport coefficient for A on the wetted part is given by

$$\frac{1}{k_{A,w}} = \frac{1}{k_{glA}} + \frac{1}{k_{lsA}} + \frac{\Delta\epsilon_1}{\sqrt{1 + \delta}\phi_y D_{Ae}} \tag{12}$$

where $\phi_y = \Delta(k_1/D_{Ae})^{1/2}$, $gl(ls)$ denotes gas-to-liquid (liquid-to-solid), and ϵ_1 is given by

$$\epsilon_1 = \frac{1}{\tanh(\sqrt{1 + \delta}\phi_y)} - \frac{1}{\sqrt{1 + \delta}\phi_y} \tag{13}$$

On the nonwetted part the expression for $k_{A,n}$ at any lateral location, say $s = s'$, depends on which of the two reactions is occurring. If both reactions occur ($s_R^* > s_B^* > s'$), then

$$\frac{1}{k_{A,n}} = \frac{1}{k_{gsA}} + \frac{\Delta\epsilon_1}{\sqrt{1 + \delta}\phi_y D_{Ae}} \tag{14}$$

where gs denotes gas-to-solid. If only reaction 2 occurs ($s_R^* > s' > s_B^*$), then

$$\frac{1}{k_{A,n}} = \frac{1}{k_{gsA}} + \frac{\Delta\epsilon_2}{\sqrt{\delta}\phi_y D_{Ae}} \tag{15}$$

where

$$\epsilon_2 = \frac{1}{\tanh(\sqrt{\delta}\phi_y)} - \frac{1}{\sqrt{\delta}\phi_y} \tag{16}$$

If neither reaction occurs ($s' > s_R^* > s_B^*$), then $k_{A,n} = k_{gsA}$, implying that in the absence of reaction there is no intraparticle resistance to the supply of A in the y direction.

A similar analysis yields the overall mass transport coefficient for B:

$$\frac{1}{k_B} = \frac{1}{k_{lsB}} + \frac{\Delta\epsilon_1}{\sqrt{1+\delta}\phi_y D_{Be}} \tag{17}$$

Analogously for R:

$$\frac{1}{k_R} = \frac{1}{k_{lsR}} + \frac{\Delta\epsilon_1}{\sqrt{1+\delta}\phi_y D_{Re}} \tag{18}$$

In deriving Eqs. 12–18 we have not considered the possibility of depletion of B or R at some point away from the surface. In a more exact analysis that accounts for depletion in the y direction, explicit expressions for Δ_i^* would not be derivable. Also, the model does not account for possible diffusive mass transport between the wetted and nonwetted regions through an inert core for surface shell catalysts. Clearly, this is justified if the core is impermeable (i.e., the washcoated catalyst). For catalysts with permeable cores this diffusion process may not be insignificant for some conditions. These points are considered later.

Selectivity and effectiveness expressions

Two catalysts performance indicators are the effectiveness η and the selectivity Σ or yield Y. For this reaction system the intrinsic selectivity of R, Σ_i, is defined as the ratio of the rate of A consumed by reaction 1 to the total rate of A consumed by both reactions:

$$\sum_i = \frac{r_{1,i}}{r_{1,i} + r_{2,i}} = \frac{1}{1+\delta} \tag{19}$$

where the subscript i denotes intrinsic and $\delta = k_2/k_1$. We note that Σ_i is bounded between unity ($\delta \to 0$) and zero ($\delta \to \infty$). The intrinsic yield, Y_i, is defined as the ratio of the net rate of R produced to the rate of B consumed by reaction 1:

$$Y_i = \frac{\nu_{R1}r_{1,i} - \nu_{R2}r_{2,i}}{\nu_B r_{1,i}} = \frac{\nu_{R1}}{\nu_B} - \frac{\nu_{R2}}{\nu_B}\delta \tag{20}$$

Y_i can have any positive or negative value, depending on the stoichiometric coefficients and δ.

The catalyst effectiveness satisfies

$$r_T = r_1 + r_2 = \eta(k_1 + k_2)C_{Ae}(V_{p,act}/V_p) \tag{21}$$

where r_T is the total A consumption rate, and $V_{p,act}/V_p$ is the ratio of the active to total pellet volume; it is less than unity for the washcoated or surface shell porous catalysts. η is defined as the ratio of the overall rate to the rate with complete wetting and no transport limitations:

$$\eta = \frac{1}{(1+\delta)\phi^2}\left[\alpha Bi_{A,w}E_w + \alpha Bi_{A,n}(1-E_w) - \alpha Bi_{A,w}\int_0^{E_w} u_{A,w}\,ds - \alpha Bi_{A,n}\int_{E_w}^1 u_{A,n}\,ds\right] \tag{22}$$

Although the integrals in Eq. 22 are over the entire wetted and nonwetted regions, the integration limits must be modified for each particular case if depletion occurs in $0 < s < 1$, Figure 2. For example, for case 6 ($0 < s_B^* < s_R^* < E_w$) the integration in the wetted zone is over the three subintervals $[0, s_B^*]$, $[s_B^*, s_R^*]$, and $[s_R^*, E_w]$.

The selectivity is the ratio of the rate of reaction 1 and total rate:

$$\sum = \frac{r_1}{r_1 + r_2} \tag{23}$$

Supplementary Material D provides the selectivity expressions for each of the ten cases. The dimensionless overall rates R_1 and R_2 satisfy

$$\eta = R_1 + R_2 = \Sigma\eta + (1-\Sigma)\eta \tag{24}$$

The yield is the ratio of the net production rate of R to the rate of B consumption by reaction 1; it is related to stoichiometric coefficients and the selectivity by

$$Y = \frac{\nu_{R1}}{\nu_B} - \frac{\nu_{R2}r_2}{\nu_B r_1} = \frac{\nu_{R1}}{\nu_B} - \frac{\nu_{R2}(1-\Sigma)}{\nu_B\Sigma} \tag{25}$$

When the yield is identically zero there is no net formation or consumption of R. If the yield is positive (negative) there is a net production (consumption) of R. For example, if all the stoichiometric coefficients are unity the yield is zero when $\Sigma = 0.5$ (i.e., $r_1 = r_2$).

Model Simulations: The Washcoated Catalyst

Base case features

In this section we examine the model predictions in order to illustrate some important features. A set of base case parameter values is provided in Table 4. This case is characterized by fast reactions and intrinsic kinetics that favor production of the reaction 1 product R ($\phi = 50$, $\delta = 0.25$), a more effective transport rate for A on the nonwetted than the wetted part ($\alpha Bi_{A2} = 100$, $\alpha Bi_{A1} = 1$), effective transport of B and R on the wetted part ($\alpha Bi_B = \alpha Bi_R = 100$), concentrations of B and R in the liquid film that are equal to the equilibrium solubility of A ($u_{Bf} = u_{Rf} = 1$), and equal diffusivities and stoichiometric coefficients of unity ($m_B = m_{R1} = m_{R2} = 1$). A nonzero R film concentration applies to pellets located at points in the reactor in which some R has been formed upstream.

In the simulations in this section it is assumed that the diffusional resistance in the y direction is negligible (the criteria of

Table 4. Parameter Values for the Base Case

Wetting efficiency	E_w between 0 and 1
Kinetic parameters	$\delta = 0.25$ $\phi = 50$
Species A parameters	$\alpha Bi_{A1} = 1$ $\alpha Bi_{A2} = 100$
Species B parameters	$\alpha Bi_B = 100$ $u_{Bf} = 1$ $m_B = 1$
Species R parameters	$\alpha Bi_R = 100$ $u_{Rf} = 1$ $m_{R1} = 1$ $m_{R2} = 1$

Eq. 2 are satisfied). With $\phi = 50$ this means that the active component is concentrated in a thin porous support layer of about 100 μm thickness on an impermeable support core. α appears always as a coefficient of each of the Biot numbers and is arbitrary. Later, the more realistic uniformly active catalyst is considered.

Figure 3a shows the dependence of the dimensionless rates R_1 and R_2 as a function of the wetting efficiency E_w. The ratio of the selectivity Σ to the intrinsic selectivity Σ_i, which is equal to 0.8, Eq. 19, and the points of B and R depletion, s_B^* and s_R^*, are plotted as a function of E_w in Figure 3b. In each graph vertical dashed lines divide the wetting efficiency into ranges for which the species B and R depletion points occur at different relative points. The regions are assigned the appropriate case number as defined in Figure 2. Note that for the chosen parameter values cases 4, 6, and 7 are not encountered. Species A, B, and R concentration profiles are plotted in Figures 4a–4e for five different E_w values corresponding to cases 1, 2, 3, 5, and 8.

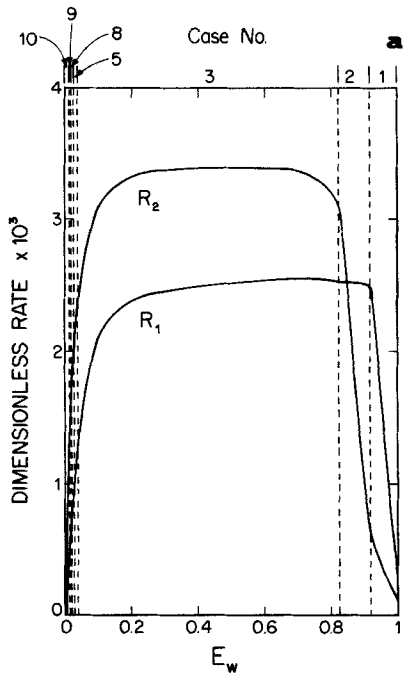

Figure 3a. Dependence of dimensionless rates on wetting efficiency.
Parameter values in Table 4

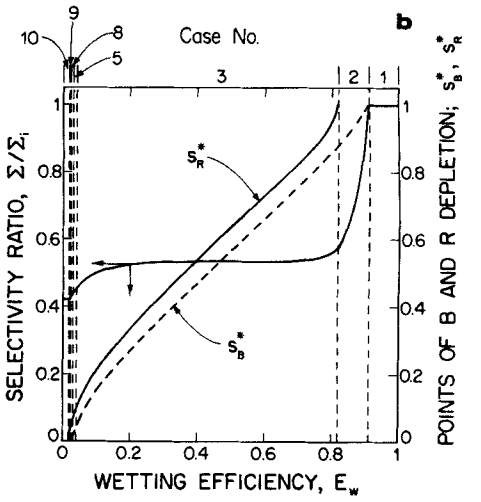

Figure 3b. Dependence of selectivity ratio and points of B and R depletion on wetting efficiency for the base case.
Parameter values in Table 4

The qualitative features of the rate dependence on the wetting efficiency are consistent with the single reaction case (Harold and Ng, 1987). The rate curves both exhibit flat maximums, implying that the rates are sustained at high levels over a wide range of wetting efficiencies. In this range an increased wetting has negligible effect on the overall rate because intraparticle diffusion is the controlling process. The rates approach zero as the wetting efficiency tends to zero since nonvolatile reactants B and R are supplied only from the liquid. The rates increase as E_w is increased from near zero because of an increased utilization of the catalyst. As $E_w \rightarrow 1$ the rates decrease because of the slower A supply rate through the wetted than the nonwetted part.

The Σ/Σ_i selectivity ratio dependence on the wetting efficiency has several key features. The actual and intrinsic selectivities are identical if both B and R are present throughout the entire pellet. This is true for wetting efficiencies exceeding 0.92 (case 1). Under these conditions the reaction rates are independent of species B and R and the network behaves as the simultaneous network $A \rightarrow R$, $A \rightarrow P$. Since the reaction kinetics are both first-order in A, the selectivity is unaffected ($\Sigma/\Sigma_i = 1$). This was shown for the single-phase simultaneous reaction network (Wheeler, 1955). Figure 4a shows the A, B, and R profiles for $E_w = 0.95$. The A concentration is virtually zero throughout the wetted part because of an ineffective supply rate. It is small within the nonwetted part because of the rapid reaction. The concentration of B remains close to its bulk value throughout most of the wetted part. It decreases as the wetted-nonwetted boundary is approached because of the increased supply of A and subsequent reaction. The R concentration increases because reaction 1 is faster than reaction 2.

For wetting efficiencies between 0.815 and 0.92 species B depletion occurs but a rapid supply and production rate of R prevent its depletion (case 2). A sharp selectivity decrease occurs in this E_w range since A can only react with R in the part of the pellet in which B is depleted. The reaction 2 rate exceeds the reaction 1 rate for E_w less than 0.84. Below this value there is

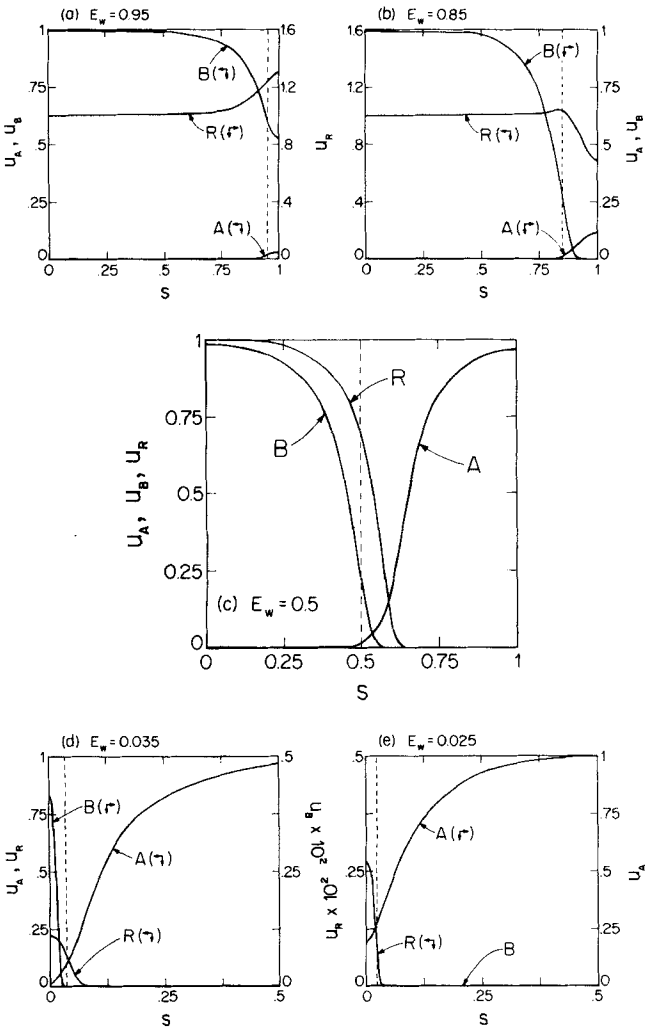

Figure 4. Base case *A*, *B*, and *R* concentration profiles for wetting efficiencies for cases 1, 2, 3, 5, and 8.
Cases defined and identified in Figures 2 and 3

a net consumption of $R(\Sigma < 0.5)$. Figure 4b shows a set of typical profiles for $E_w = 0.85$. The A profile resembles that in Figure 4a. In this case the nonwetted zone is wide enough to provide a sufficient supply of A to deplete B in the nonwetted part. Within the region of B depletion R is consumed rapidly so that its profile exhibits a local maximum within the nonwetted part. This demonstrates the detrimental impact of the slow R diffusion and its nonvolatility, both of which prevent it from escaping before it reacts further with A to form the undesired product P.

Depletion of species R occurs if the wetting efficiency is reduced below 0.815. For a large E_w range—between 0.04 and 0.815—species B and R deplete in the nonwetted part of the pellet (case 3). Figure 4c shows representative profiles for $E_w = 0.5$. The ineffective supply rate of A from the liquid limits the extent of reaction in the wetted part. The comparatively effective A supply rate in the nonwetted region provides ample A for reaction. The local consumption rate of A is highest in the nonwetted part of the pellet in which B and R are not depleted. The slow intraparticle diffusion of B and R relative to the reaction rates prevents a complete utilization of the nonwetted region, and B and R deplete. For E_w between 0.2 and 0.7 the selectivity is insensitive to E_w changes ($\Sigma/\Sigma_i = 0.52$). In this range, a variation in E_w shifts the location, but not the size, of the intrapellet zone in which the local reaction rates are highest.

As E_w is decreased from 0.04 to near zero the rates decrease significantly as the points of B and R depletion tend to zero. For E_w between 0.034 and 0.04, $B(R)$ depletes in the wetted (nonwetted) part (case 5). Under these conditions the supply and diffusion of B are ineffective, resulting in complete depletion of B in part of the wetted zone. Figure 4d shows a representative set of profiles for this case with $E_w = 0.035$. Note that $B(R)$ depletion in the wetted (nonwetted) parts. For E_w below 0.034, B is completely consumed and cases 8, 9, and 10 are encountered. Figure 4e shows the profiles for $E_w = 0.025$, which corresponds to the depletion of R in the nonwetted part (case 8). For E_w below 0.02 both B and R are completely depleted. In this range the selectivity is constant and dependent only on the external mass transfer coefficients, film concentrations, and stoichiometries. Since the supply rates of B and R are both proportional to the area of wetted catalyst surface (i.e., E_w) there is no dependence on E_w, Eq. 23.

Impact of physical parameters: Selectivity dependence on wetting efficiency

In this section the influence of some transport and kinetic parameters on the desired product (R) selectivity-wetting efficiency dependence is examined. An objective is to determine the value or range of a particular parameter that expands the wetting efficiency range over which the selectivity is sustained at a high level. Since the selectivity can never exceed its intrinsic value these conditions correspond to those that give the intrinsic selectivity. Of particular interest is the minimal wetting efficiency—if it exists—that give the intrinsic selectivity for a given set of parameters. To address these questions a family of curves of the selectivity-intrinsic selectivity ratio (Σ/Σ_i) as a function of the wetting efficiency (E_w) are constructed for several values of one parameter. Important trends are printed in *italics*. The parameters to be checked are:

1. The species A mass transfer coefficient αBi_{A1}, αBi_{A2}
2. The species B mass transfer coefficient and bulk concentration αBi_B, u_{Bf}
3. The species R mass transfer coefficient and bulk concentration αBi_R, u_{Rf}
4. The catalytic activity ϕ
5. The reaction stoichiometries m_B, m_{R1}, m_{R2}

Again, the simulations apply to a catalyst with a thin active layer on an impermeable core. Thus, variations in the overall transport coefficients are not adjusted for changes in δ, ϕ, and α according to Eqs. 12–18. However, as demonstrated later, the qualitative results are applicable to cases in which intraparticle limitations in the direction normal to the wetted surface cannot be ignored.

1. Volatile Reactant (A) Mass Transfer Coefficients. The impacts of the dimensionless mass transport coefficient for A on the wetted (αBi_{A1}) and nonwetted (αBi_{A2}) parts on the selectivity-wetting efficiency dependence are shown in Figures 5 and 6, respectively. Their influences are quite different.

An intermediate A supply rate from the liquid gives a maximum selectivity for a wide intermediate range of wetting efficiencies. An increase in αBi_{A1} from zero to an unbounded value

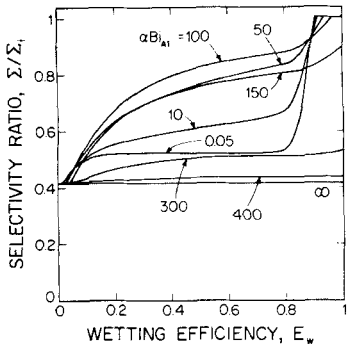

Figure 5. Dependence of selectivity ratio on E_w for various αBi_{A1} values.

results in a nonmonotonic variation in the selectivity for E_w between 0.06 and 0.9.

For $E_w < 0.02$ the selectivity is independent of αBi_{A1} since the supplies of B and R are the limiting processes; i.e., B and R are completely depleted, and Σ is independent of E_w. This is true even for $\alpha Bi_{A1} \rightarrow 0$ because a sufficient supply of A diffuses from the nonwetted part to consume completely the B and R in the thin wetted zone. Within the narrow E_w range of 0.02 to 0.05, Σ is a monotonic decreasing function of αBi_{A1}. In this range the wetted zone is sufficiently wide to prevent the complete consumption of B and R as $\alpha Bi_{A1} \rightarrow 0$. An increasing A supply rate from the liquid increases the amount of R that is consumed to P, and hence reduces the selectivity.

For E_w between 0.06 and 0.9 this trend is reversed. In this range there exists an αBi_{A1} value that maximizes the selectivity. This is a result of two competing effects. For small αBi_{A1} much of the B that is supplied is not consumed in the wetted part because of the ineffective A supply rate on the wetted part and the sufficiently wide liquid film. Thus, a large amount of B diffuses into the nonwetted part and is consumed. The R that is produced cannot escape before being consumed itself because of its slow intraparticle diffusion and its nonvolatility. The intraparticle diffusion control is evidenced by the flat part of the $\alpha Bi_{A1} = 0.05$ curve. As αBi_{A1} is increased, more B is consumed in the wetted zone. Thus, more R is produced in the wetted zone and escapes before reacting further. However, if αBi_{A1} is increased further and eventually becomes unbounded (above 100 in this case) depletion of B occurs within an increasing portion of the wetted part. A more rapid consumption of R occurs in this portion of the pellet, and the selectivity decreases. In the limit of $\alpha Bi_{A1} \rightarrow \infty$ complete consumption of B and R occurs and Σ attains its complete depletion value for all E_w.

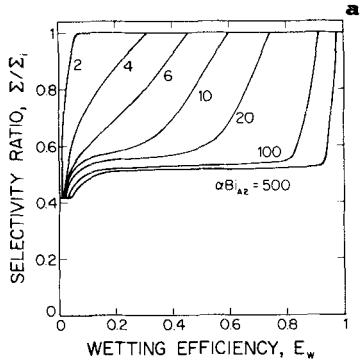

Figure 6a. Dependence of selectivity ratio on E_w for various αBi_{A2} values.

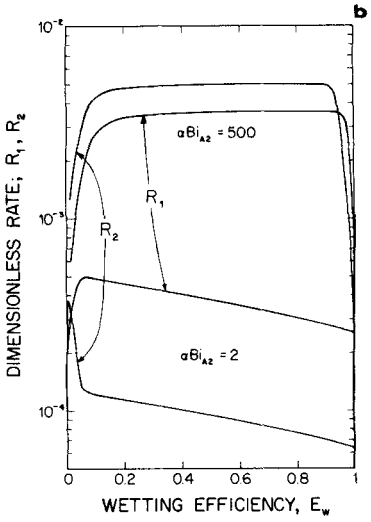

Figure 6b. Dependence of dimensionless rates of reactions 1 and 2 on E_w for $\alpha Bi_{A2} = 2$ and 500.

For $E_w > 0.9$, Σ/Σ_i is a decreasing function of αBi_{A1}. For $\alpha Bi_{A1} \rightarrow 0$, $\Sigma/\Sigma_i = 1$ (no B or R depletion), and for $\alpha Bi_{A1} \rightarrow \infty$, Σ/Σ_i approaches the complete depletion limiting value. This trend demonstrates that a slow A supply rate from the wetted zone permits B and R to diffuse throughout the entire nonwetted region for a sufficiently large E_w. However, an infinite supply rate of A consumes all the B supplied and R supplied and formed.

The influence of αBi_{A2} is less complex, Figure 6a. An increase in αBi_{A2} to 500 from its base case value of 100 reduces somewhat the selectivity for all wetting efficiencies except for $E_w \rightarrow 0$, the complete depletion limit, and $E_w \rightarrow 1$, the no-depletion limit. These two regimes are connected by a third intraparticle diffusion controlled regime in which the selectivity is essentially constant. On the other hand, decreases in αBi_{A2} from 100 to near zero increase the selectivity to its intrinsic value for all E_w. This is because a reduced A supply rate from the gas results in lower consumption rates of B and of the desired product R within the nonwetted zone. *In the limit of a negligible* A *supply rate from the nonwetted part* B *and* R *can diffuse to all points and the selectivity attains its intrinsic value.*

From these findings, one may conclude that an increased gas-to-solid mass transfer resistance is beneficial since it results in the reduction of the minimal wetting efficiency necessary to achieve the intrinsic selectivity. However, this benefit is not achieved without a penalty. The selectivity enhancement is accompanied by a reduced production of R. Figure 6b shows a plot of the dimensionless rates as a function of E_w for $\alpha Bi_{A2} = 2$ and 500. When $\alpha Bi_{A2} = 2$, R_1 exceeds R_2 for all $E_w > 0.02$. When $\alpha Bi_{A2} = 500$, R_2 exceeds R_1 for all $E_w < 0.94$. However, for the $\alpha Bi_{A2} = 2$ case the absolute rates are about one order of magnitude less at all wetting levels. *Thus, there is a trade-off between selectivity enhancement accompanied by low overall rates with ineffective species* A *gas-to-solid mass transport, and lower selectivities accompanied by increased rates with an effective gas-to-solid mass transport.*

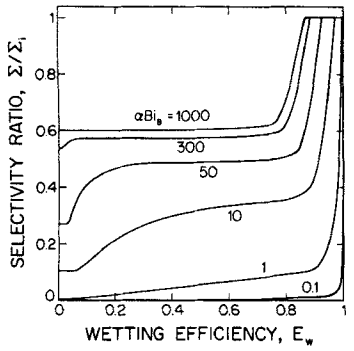

Figure 7. Dependence of selectivity ratio on E_w for various αBi_B values.

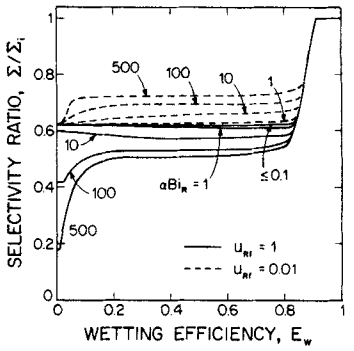

Figure 9. Dependence of selectivity ratio on E_w for various αBi_R values.

2. Nonvolatile Reactant (B) *Mass Transfer Coefficient and Film Concentration.* The impacts of αBi_B and u_{Bf} on the selectivity-wetting efficiency relationship are shown in Figures 7 and 8, respectively. Variations in αBi_B and u_{Bf} correspond to proportional changes in the species B liquid-to-solid mass transfer coefficient and its average liquid film concentration, respectively. The model predicts that *an increase in the* B *supply* (αBi_B, u_{Bf}) *to a larger fraction of the catalyst increases the selectivity of* R *at all wetting efficiencies. The selectivity increases are accompanied by overall rate increases. An increase in* αBi_B *and* u_{Bf} *also decreases the minimal* E_w *necessary to give the intrinsic selectivity.*

In the regime of a B supply rate limited reaction 1, which corresponds to αBi_B and u_{Bf} approaching zero, the selectivity is low because of a small R production rate by reaction 1 and a rapid R consumption rate by reaction 2. For sufficiently small E_w, B is completely depleted. Increases in αBi_B and u_{Bf} from values near zero supply B to a larger fraction of the pellet. As a result, reaction 1 occurs in a larger fraction of the pellet and the selectivity increases.

A net production of R *requires a high species* B *liquid-to-solid mass transfer coefficient and liquid film concentration if* R *is being supplied competitively (i.e.,* $u_{Rf} > 0$*).* Figure 7 shows that an increase in αBi_B even to 1,000 does not result in a net production of R if R depletes within the pellet ($E_w < 0.77$), as Σ is always less than 0.5 in this range of E_w. The reason is that the sufficiently large R film concentration ($u_{Rf} = 1$) prevents the transport of a fraction of the produced R from the pellet before it reacts further to P. There is a net production of R only if more R leaves the pellet than enters from the liquid film ($u_{Bf} > 5$ in Figure 8).

3. Nonvolatile Intermediate (R) *Mass Transfer Coefficient and Film Concentration.* The influence of αBi_R and u_{Rf} on the selectivity-wetting efficiency relationship is shown in Figures 9 and 10, respectively. An increase in u_{Rf} increases the supply of R to the pellet, as u_{Rf} is proportional to the average liquid film concentration of R. An increase in αBi_R increases(decreases) the amount of R if the film concentration of R is sufficiently large(small). The trend is that *the selectivity decreases if the amount of* R *supplied to the pellet* (u_{Rf}) *increases and* R *depletes at some point within the pellet. The impact of the* R *transport coefficient* (αBi_R) *depends on the magnitude of the species* R *film concentration; for low* u_{Rf} *an increase in* αBi_R *increases the selectivity; for high* u_{Rf} *an increase in* αBi_R decreases the selectivity.

There are two more specific features shared by both plots, Figures 9, 10. First, the selectivity is independent of E_w as $E_w \to 0$ because both B and R deplete completely, conditions for which Σ is independent of E_w. Second, each curve intersects and follows a single locus for sufficiently large E_w. The locus monotonically increases until it intersects the $\Sigma/\Sigma_i = 1$ line at an E_w value less than unity. An individual curve merges with the locus at the E_w for which the point of R depletion is equal to unity ($s_R^* = 1$). For wetting efficiencies exceeding this value the selectivity is independent of that particular species R parameter since there is no rate dependence on R. As the supply of R is decreased a higher E_w is necessary to supply R throughout the catalyst.

Some features that are unique to each plot are now highlighted. *An increase in the species* R *mass transport coefficient*

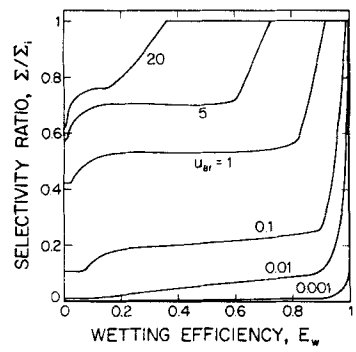

Figure 8. Dependence of selectivity ratio on E_w for various u_{Bf} values.

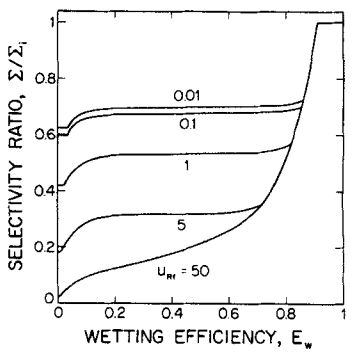

Figure 10. Dependence of selectivity ratio on E_w for various u_{Rf} values.

(αBi_R) reduces the selectivity at all wetting efficiencies if the liquid film concentration of R *is sufficiently large and* R *depletes within the pellet* (solid lines in Figure 9). Pellets located sufficiently downstream in the reactor will be exposed to a liquid that contains an appreciable amount of the intermediate species R. If u_{Rf} is sufficiently large, in reducing the mass transport resistance R will enter such pellets more rapidly from the liquid film. Since reaction 2 is rather fast ($\delta\phi^2 = 625$) the R that enters is rapidly converted to P within the part in which B is depleted. This is detrimental to the selectivity. As αBi_R is decreased toward zero (<0.1) R cannot enter or leave the liquid film. Any R produced by reaction 1 is consumed by reaction 2, thus producing P. As long as the reactions are sufficiently fast to depleted B and R within the pellet, there is no net consumption or production of R, and the overall yield is zero ($\Sigma/\Sigma_i = 0.625$). A curious result was found for intermediate αBi_R values—the existence of a shallow local minimum in the Σ/Σ_i vs. Σ_w curve. This indicates that the selectivity obtained in the external mass transport controlled regime is slightly higher than that in the intraparticle diffusion controlled regime.

On the other hand, an increasing αBi_R is beneficial to the selectivity if the concentration of R in the film is sufficiently small. This is the case for pellets near the reactor entrance with a liquid feed containing only B. *An increase in* αBi_R *increases the selectivity at all wetting efficiencies if the liquid film concentration of* R *is sufficiently small and* R *depletes within the pellet.* Figure 9 shows for $u_{Rf} = 0.01$ (dashed lines) that a variation in αBi_R from near zero to 500 increases the selectivity. In this case a reduced transport resistance for R is beneficial since this facilitates a more rapid removal of R from the pellet. There is a transport of R out of the pellet at all points (s) for which $u_R > u_{Rf}$ (=0.01). As for the $u_{Rf} = 1$ case, as $\alpha Bi_R \rightarrow 0$, R does not exchange with the liquid film, and $\Sigma = 0.5$ for all E_w less than the value at which $s_R^* = 1$.

An increasing u_{Rf} has a detrimental effect on the selectivity, Figure 10. Because of the active catalyst the supplied R is rapidly converted to P. Only for sufficient small u_{Rf} (<0.1) is there a net production of R. This illustrates that the concentration of R in the liquid film is a key variable in determining whether R is net consumed or produced.

4. Catalytic Activity. The effect of the catalytic activity which is determined by varying the Thiele modulus ϕ. The selectivity dependence on the wetting efficiency is shown in Figure 11 for several ϕ values. *As the Thiele modulus ϕ decreases the overall rates become limited by the reaction rates and the selectivity approaches its intrinsic value. In this case an increase in the selectivity is accompanied by an increase in the overall catalyst effectiveness.* For small values of ϕ the intrinsic reaction rates are slower than the mass transport processes (solid lines in Figure 11). This permits species B and R to more easily diffuse to a larger fraction of the pellet without being consumed. Thus, a smaller wetting efficiency is required to supply B and R to all points in the catalyst as ϕ decreases; i.e., $\Sigma < \Sigma_i$ over a progressively smaller E_w range.

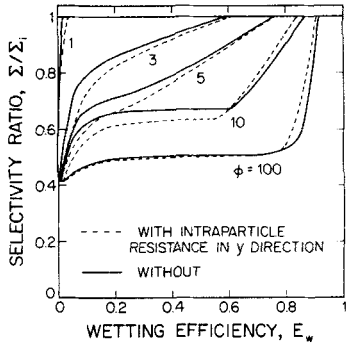

Figure 11. Dependence of selectivity ratio on E_w for various ϕ values.

5. Stoichiometry. The reaction stoichiometries can also have a significant impact on the selectivity as revealed by variations in m_B, m_{R1}, and m_{R2}. Simulations reveal that increases in m_B^{-1} (reciprocal of m_B), corresponding to decreases in ν_B, result in the same qualitative trends in the selectivity vs. wetting efficiency curves as αBi_B and u_{Bf} are increased. Increases in m_{R1}^{-1} and m_{R2} have the same qualitative effect as increases in u_{Bf}.

Impact of Intraparticle Diffusional Resistance in the *y* Direction: The Uniformly Active Catalyst

Up to now we have not accounted explicitly for possible intraparticle diffusional gradients in the direction normal (y) to the wetted surface. These are not negligible if either criterion in Eq. 2 is violated. In this section some model predictions are presented for the more realistic porous catalyst of uniform activity in which diffusional gradients in two directions exist. For catalysts with volume V_p and external area S_x, the effective aspect ratio is given by $\alpha = (S/2)/(V_p/S_x)$ and is typically on the order of 1–10. The approximate scheme, which incorporates the intraparticle resistances into the overall mass transport coefficients according to the scheme outlined earlier, is employed. Simulations of the concentration profiles, effectiveness, and selectivity use the same model solutions. However, the overall Biot numbers are functions of the external mass transfer coefficients (i.e., $Bi^o_{A,w}$, $Bi^o_{A,n}$, Bi^o_B, Bi^o_R), the aspect ratio α, the rate constant ratio δ, and the Thiele modulus ϕ according to Eqs. 12–18.

Using this prescription, the computed selectivity ratio dependence on E_w is shown in Figure 11 as the dashed lines for several ϕ values. The external mass transport coefficients are assigned the values $Bi^o_{A,w} = 0.2$, $Bi^o_{A,n} = 20$, $Bi^o_B = 20$, and $Bi^o_R = 20$, and the aspect ratio α is equal to 5. These values are used so that in the limit of negligible y-directed intraparticle diffusion limitations we satisfy $\alpha Bi_{A,w} = \alpha Bi^o_{A,w} = 1$, $\alpha Bi_{A,n} = \alpha Bi^o_{A,n} = 100$, $\alpha Bi_B = \alpha Bi^o_B = 100$, and $\alpha Bi_R = \alpha Bi^o_R = 100$, Eqs. 12–18. Thus, the model predictions without accounting for the y-directed diffusional resistance should match model predictions that account for the resistance as the resistance becomes insignificant (e.g., as the thickness of the active zone gets very small). By comparing the deviation between the solid and dashed curves for a fixed ϕ, Figure 11, the impact of the additional resistance is determined.

The negligible deviation for $\phi = 1$ simply shows that the overall rates are reaction controlled so that the additional resistance has little effect.

In the case of a rapid reaction ($\phi = 100$) the additional resistance has a more complex effect. For sufficiently small E_w the external supply of B and R limits the overall rates and depletion of B and R occurs within the wetted zone. For $E_w \rightarrow 0$, complete depletion of B and R occurs, and the selectivity attains its lower bound value. Thus, for small E_w the additional intraparticle resistance has little if any effect. For intermediate E_w, between approximately 0.2 and 0.8, the diffusional resistance in the lat-

eral (x) direction and the rapid reactions prevent B and R from diffusing very far into the nonwetted part. The additional resistance shifts the points of B and R depletion further into the nonwetted zone, but the relative overall rates are only slightly altered. This insensitivity is a result of the external transport resistance of A supply to the pellet from the liquid film being the dominant one in the y direction. Inspection of Eqs. 12 and 15 reveals that for large ϕ_y (equal to 20 in this case) the intraparticle resistance term is negligible compared to the external resistance terms. Such a shift from intraparticle to external transport control as the catalytic activity is increased is encountered in single-phase catalytic reactions (Froment and Bischoff, 1979). For E_w exceeding 0.75 the model predicts a higher selectivity for the case with the additional resistance. This means that somewhat less B is consumed in the wetted part, enabling it to diffuse further into the nonwetted zone before being depleted. Thus, a smaller E_w is required to supply B and R to all points in the pellet. Even with the additional resistance, the model predicts that above a critical wetting efficiency there is no depletion of B and R within the pellet, and the selectivity is equal to its intrinsic value. This is a result of the more effective supply of B than A from the liquid film covering most of the surface. It should be pointed out that in not accounting for B and R depletion in the y direction, the approximate scheme may overpredict the selectivity for very rapid reactions.

For the intermediate values of ϕ the overall rates are neither reaction controlled nor severely limited by external transport. There is a more significant effect of the y-directed intraparticle diffusional resistance. Inspection of the $\phi = 3$, 5, and 10 curves reveals a selectivity decrease for $E_w < 0.6$. The principle cause for the decrease is that the y-directed diffusional resistance reduces the total amount of A and B that react, thus reducing the amount of R produced. Also, the R that is produced cannot escape as easily in the part of the wetted zone where $u_R > u_{Rf}$, and is subsequently converted to P. A secondary effect is a reduced supply rate of R from the liquid film to the part of the pellet where $u_{Rf} > u_R$, which tends to increase the selectivity, Figure 9. However, since reaction 1 is four times as fast as reaction 2, the former effects dominate. This was confirmed by checking some concentration profiles. Figure 12 shows the impact of the additional resistance on the overall rates of both reactions as a function of E_w for $\phi = 10$. The overall rates are reduced by between 15 and 75%. These results demonstrate the detrimental impact of the diffusional limitations in the y direction on both the overall rates and selectivity.

The dependence of the selectivity ratio on the aspect ratio for four different wetting efficiencies is shown in Figure 13. Model solutions with (solid line) and without (dashed line) diffusional limitations in the y direction are compared. The external components of the overall Biot numbers are assigned the values $Bi^o_{A,w} = 0.1$, $Bi^o_{A,n} = 10$, $Bi^o_B = 10$, and $Bi^o_R = 10$. The remaining parameters assume their base case values, Table 4. Only aspect ratios exceeding 5 are considered since smaller values stretch the geometric applicability of the model. The selectivity ratio is a monotonic increasing function of α both with and without accounting for y-directed diffusional limitations. For the model not accounting for the additional resistance the increase implies that a fixed external supply rate of reactants (A, B, R) is made over a thinner active zone. This reduces the external mass transport resistance. The y-directed diffusional limitations reduce the selectivity for all α values, with the decrease more significant for smaller E_w. This follows from the discussion related to Figure 11. For a given E_w, as the active zone thickness is decreased (α increased) the selectivity approaches the value predicted by the model without accounting for the additional intraparticle resistance. This expected result demonstrates that for progressively thinner active zones this resistance becomes negligible.

Discussion and Conclusions

A one-dimensional model has been developed to describe diffusion and reaction in a partially wetted catalytic pellet in which a consecutive-parallel reaction network occurs. The model predicts that depletion of one or both nonvolatile liquid reactants lowers the desired product selectivity below its intrinsic level. This shift within the pellet from volatile reactant limited to nonvolatile reactant limited reactions is a complex function of the stoichiometry of the interacting reactions, the intraparticle mass transport, and the external mass transport and reaction kinetics, both of which are spatially discontinuous because of the partial wetting and the assumed kinetic rate model, respectively. This study points out the need to use bimolecular kinetic rate expressions in properly predicting the shift in limiting reactants within the partially wetted pellet. The complex transport-reaction interactions and liquid reactant depletion effect result in not-

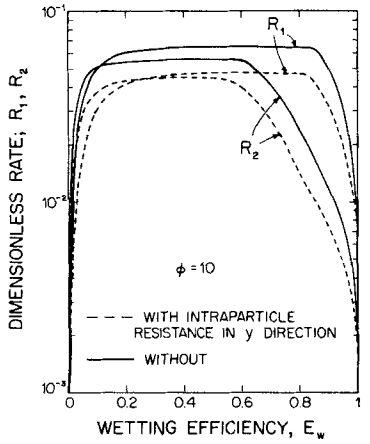

Figure 12. Dependence of dimensionless reaction rates on E_w for $\phi = 10$ (Figure 11).

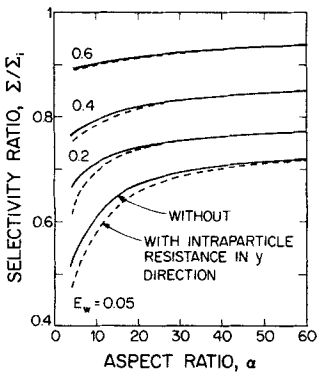

Figure 13. Dependence of selectivity ratio on aspect ratio for several wetting efficiencies.

Assumed parameter values: $Bi^o_{A1} = 0.1$, $Bi^o_{A2} = 10$, $Bi^o_B = 10$, $Bi^o_R = 10$

Remaining parameters assume their base case values, Table 4

obvious, sometimes surprising trends in the selectivity dependence on the wetting efficiency. Only the rather detailed analysis is able to isolate the many subtle points. Model verification awaits single partially wetted pellet data.

The model predicts that in most cases a minimal wetting efficiency exists above which the intrinsic selectivity is attained. However, because the overall rates either increase or exhibit a maximum as the wetting efficiency is increased, selectivity improvements do not always synchronize with overall rate increases. In these cases the optimal wetting efficiency range is determined by a trade-off between a high overall rate, low selectivity state, or a lower overall rate, high selectivity state. The size of this range depends on the particular reaction system and operating conditions.

The model is formally valid for washcoated catalysts with a sufficiently thin active layer. An approximate method of accounting for intraparticle diffusion in the direction (y) normal to the wetted surface permits the model to describe uniformly impregnated catalyst pellet performance. The model also assumes a first-order dependence on the dissolved gas reactant and a zero-order dependence on the liquid reactants. However, the zero-order dependence with the depletion effect accounted for is a first step toward modeling reactions that have bimolecular rate forms. A key advantage of the one-dimensional formulation with simplified kinetics is the significantly more efficient means of predicting catalyst performance; i.e., its use involves the simultaneous solution of one or two nonlinear algebraic equations. The accuracy of the model predictions and validity of the assumptions can only be checked by comparison with the numerical solution predictions of the two-dimensional model with more realistic kinetics. However, this is by no means a trivial numerical task, especially for highly active catalysts (Funk et al., 1988). Thus, there is a trade-off between computational efficiency and predictive accuracy.

The model also assumes the existence of a single film of constant width and thickness, a completely liquid-filled pore volume, nonvolatile liquid reactants and products, and negligible heat effects. The existence of multiple rivulets, partial pore fill-up, and vaporization raises intriguing questions with regard to selectivity in multiple gas-liquid catalytic reaction systems. It is clear that additional experimental and modeling studies are needed to address these problems.

This study is a necessary step in determining how the imperfect wetting influences the overall selectivities in a trickle-bed reactor. There are several key points with regard to trickle-bed design and operation. First, the common assumption that one or more of the reactants are in excess throughout the pellet may not be valid for some pellets in the reactor. This may lead to pitfalls in designing the reactor to maximize the desired product selectivity.

Second, selectivity is improved by feeding a large concentration of the reaction 1 nonvolatile reactant B in order to provide an excess of B throughout the reactor. The principal reason for the departure in selectivity from the intrinsic level is the existence of an intrapellet region wherein the liquid reactant B is depleted and the desired product R is consequently rapidly converted to P. A large B supply would provide an excess of B within the entire pore volume of even slightly wetted pellets, thus minimizing this detrimental depletion effect.

Third, selectivity is improved by wetting the pellets as completely as possible. The complete wetting prevents liquid reactant depletion for pellets with a sufficiently thin active shell and low activity. Unfortunately, the liquid film deters the transport of the gas reactant A and hence reduces the overall rates. Thus, a window of wetting efficiencies exists for which the production rate of R is maximized. The size of this window will vary along the length of the reactor because of the changing liquid-phase composition. Thus, the prescription for optimizing the overall reactor scale production rate of R is nontrivial. At the very least, the sensitivity of selectivity and overall rates to the wetting efficiency emphasizes the need to incorporate these single pellet features into the reactor model for further analysis.

Acknowledgment

This research was partially supported by National Science Foundation Grant No. CBT-8700554. I am grateful for the helpful comments of my colleague Ka Ng.

Notation

A = gaseous reactant
B = liquid reactant
Bi_i = overall Biot number for species i
Bi_i^o = external component of Biot number for species i
C_i = liquid-phase concentration of species i
$\hat{C}_{iy}$ = liquid-phase concentration of species i, ignoring x direction
C_{iy} = average (w/r y direction) species i concentration ignoring x direction
D_{ie} = effective diffusivity of species i
E_w = wetting efficiency
$F_{i,j}$ = jth function of point(s) of depletion of ith case (Supplementary Material C)
k_i = rate constant of reaction i
$k_{i,j}$ = overall mass transport coefficient of species i in region j
k_{ij}^o = external component of $k_{i,j}$
L = pellet length
m_B = parameter, Eq. 9
m_B, m_{R1}, m_{R2} = parameters, Eq. 9
P = liquid product of reaction 2
r_j = overall rate of reaction j
$r_{j,i}$ = intrinsic rate of reaction j
$r_{k,n}$ = consumption rate of species k (A, B, or R) in nonwetted part, Table 2
$r_{k,w}$ = consumption rate of species k (A, B, or R) in wetted part, Table 2
R = liquid product (reactant) of reaction 1(2)
R_i = dimension rate of reaction j, Eq. 24
s = dimensionless lateral (x) distance
s_B^*, s_R^* = points of B and R depletion
S = pellet width
S_x = external pellet area
u_i = dimensionless concentration of species i, Eq. 9
V_p = pellet volume
x = lateral length coordinate
y = length coordinate normal to wetted surface
Y, Y_i = overall and intrinsic yield, Eqs. 20, 25
z = coordinate in direction of flow

Greek letters

α = aspect ratio of pellet, Eq. 9
δ = rate constant ratio, Eq. 9
Δ = thickness of active zone, Figure 1
Δ_i^* = effective diffusion length of species i, Eq. 10
η = effectiveness, Eq. 22
ν = stoichiometric coefficient
Σ, Σ_i = actual and intrinsic selectivity, Eqs. 23, 19
ϕ = Thiele modulus, Eq. 9
ϕ_y = Thiele modulus based on active zone thickness

Subscripts

act = active
A = species A
B = species B
e = effective, equilibrium
f = film
gl = gas-to-liquid
gs = gas-to-solid
i = intrinsic, ith element, species, region, etc.
ls = liquid-to-solid
n = nonwetted
p = pellet
R = species R
s = surface
w = wetted
y = with respect to distance coordinate normal to wetted surface
1, 2, 3, 4 = region number

Superscripts

* = point of depletion, effective diffusion length
o = external component of transport coefficient

Literature Cited

Aris, R., *The Mathematical Theory of Diffusion and Reaction in Permeable Catalysts*, v. 1, Oxford (1975).

Beaudry, E., M. P. Dudukovic, and P. Mills, "Trickle-Bed Reactors: Liquid Diffusional Effects in a Gas Limited Reaction," *AIChE J.*, **33,** 1435 (1987).

Broderick, D. H., and B. C. Gates, "Hydrogenolyses and Hydrogenation of Dibenzothiophene Catalyzed by Sulfided CoO-MoO_3/Al_2O_3: The Reaction Kinetics," *AIChE J.*, **27,** 663 (1981).

Butt, J., "Internal Mass and Heat Transport Effects on Catalytic Behavior—Activity, Selectivity, and Yield in a Complex Reaction System," *Chem. Eng. Sci.*, **21,** 275 (1966).

Dassori, C. G., J. A. Deiber, and A. E. Cassano, "Mass Transfer with Chemical Reaction in Partially Wetted Flat Plate Catalyst Pellets: Rivulet Flow Analysis," *Chem. Eng. Commun.*, **51,** 105 (1987).

Ding, J. S., S. Sharma, and D. Luss, "Steady State Multiplicity and Control of the Chlorination of Liquid *n*-Decane in an Adiabatic Continuously Stirred Tank Reactor," *Ind. Eng. Chem. Fundam.*, **13,** 76 (1974).

Froment, G. F., and K. B. Bischoff, *Chemical Reactor Analysis and Design*, Wiley, New York (1979).

Funk, G., M. P. Harold, and K. M. Ng, "Effectiveness of a Partially Wetted Catalyst for Bimolecular Reaction Kinetics," *AIChE J.* (May, 1988).

Gabitto, J. F., M. A. Laborde, and N. O. Lemcoff, "Effectiveness Factor and Selectivity for Partially Wetted Catalyst Pellets in a Parallel Reaction System," *Lat. Am. J. Heat Mass Transfer*, **9,** 75 (1986).

Gates, B. C., J. R. Katzer, and C. G. A. Schuit, *Chemistry of Catalytic Processes*, McGraw-Hill, New York (1979).

Gianetto, A., G. Baldi, V. Specchia, and S. Sicardi, "Hydrodynamics and Solid-Liquid Contacting Effectiveness in Trickle-Bed Reactors," *AIChE J.*, **24,** 1087 (1978).

Goto, S., A. Lakota, and J. Levec, "Effectiveness Factors of *n*th-Order Kinetics in Trickle-Bed Reactors," *Chem. Eng. Sci.*, **36,** 157 (1981).

Harold, M. P., and K. M. Ng, "Effectiveness Enhancement and Reactant Depletion in a Partially Wetted Catalyst," *AIChE J.*, **33,** 1448 (1987).

Hashimoto, K., M. Teramoto, T. Nagayasu, and S. Nagata, "The Effects of Mass Transfer on the Selectivity of Gas-Liquid Reactions," *J. Chem. Eng. Japan*, **1,** 132 (1968).

Herskowitz, M., "Wetting Efficiency in Trickle-Bed Reactors. The Overall Effectiveness Factor of Partially Wetted Catalyst Particles," *Chem. Eng. Sci.*, **36,** 1099 (1981a).

———, "Effect of Wetting Efficiency on Selectivity in a Trickle-Bed Reactor," *Chem. Eng. Sci.*, **36,** 1665 (1981b).

Herskowitz, M., R. G. Carbonell, and J. M. Smith, "Effectiveness Factor and Mass Transfer in Trickle-Bed Reactors," *AIChE J.*, **25,** 272 (1979).

Kale, S. S., R. V. Chaudhari, and P. A. Ramachandran, "Butynediol Synthesis. A Kinetic Study," *Ind. Eng. Chem. Prod. Res. Dev.*, **20,** 309 (1981).

Kawakami, K., and K. Kusunoki, "The Effects of Intraparticle Diffusion on the Yield of the Liquid-Phase Hydrogenation of Phenylacetylene in Stirred Basket Reactor," *J. Chem. Eng. Japan*, **9,** 469 (1976).

Kawakami, K., Y. Ohgi, and K. Kusunoki, "The Individual and Competitive Hydrogenations of Ethylene and Propylene in a Stirred Slurry Reactor," *J. Chem. Eng. Japan*, **9,** 475 (1976).

Kohler, M. A., and W. Richarz, "Experimental Study of a Complex Catalytic Reaction Network in a Trickle-Bed Reactor," *Chem. Eng. Commun.*, **41,** 59 (1986).

Lin, K., and M. M. Lih, "Concentration Distribution, Effectiveness Factor, and Reactant Exhaustion for Catalytic Reaction with Volume Change," *AIChE J.*, **17,** 1234 (1971).

Marangozis, J., O. B. Keramidas, and G. Paparisvas, "Rate and Mechanism of Hydrogenation of Cottonseed Oil in Slurry Reactors," *Ind. Eng. Chem. Process Des. Dev.*, **16,** 361 (1977).

Mills, P. L., and M. P. Dudukovic, "A Dual-Series Solution for the Effectiveness Factor of Partially Wetted Catalysts in Trickle-Bed Reactors," *Ind. Eng. Chem. Fundam.*, **18,** 139 (1979).

Mochizuki, S., and T. Matsui, "Selective Hydrogenation and Mass Transfer in a Fixed-Bed Catalytic Reactor with Gas-Liquid Cocurrent Upflow," *AIChE J.*, **22,** 904 (1976).

Ng, K. M., "A Model for Flow Regime Transitions in Cocurrent Downflow Trickle-Bed Reactors," *AIChE J.*, **32,** 115 (1986).

Ramachandran, P. A., and J. M. Smith, "Effectiveness Factors in Trickle-Bed Reactors," *AIChE J.*, **25,** 538 (1979).

Ring, Z. E., and R. W. Missen, "Trickle-Bed Reactors: Effect of Wetting Geometry on Overall Effectiveness Factor," *Can. J. Chem. Eng.*, **64,** 117 (1986).

Roberts, G., "The Selectivity of Porous Catalysts: Parallel Reactions," *Chem. Eng. Sci.*, **27,** 1409 (1972).

Ruecker, C. M., R. K. Hess, and A. Akgerman, "Effect of Partial Wetting on Scale-up of Laboratory Trickle-Bed Reactors," *Chem. Eng. Commun.*, **49,** 301 (1986).

Sakornwimon, W., and N. D. Sylvester, "Effectiveness Factors for Partially Wetted Catalysts in Trickle-Bed Reactors," *Ind. Eng. Process. Des. Dev.*, **21,** 16 (1982).

Sato, Y., T. Hirose, F. Takahashi, M. Toda, and Y. Hashiguchi, "Flow Pattern and Pulsation Properties of Cocurrent Gas-Liquid Downflow in Packed Beds," *J. Chem. Eng. Japan*, **6,** 315 (1973).

Satterfield, C. N., "Trickle-Bed Reactors, *AIChE J.*, **21,** 209 (1975).

Satterfield, C. N., and S. H. Yang, "Catalytic Hydrodenitrogenation of Quinoline in a Trickle-Bed Reactor. Comparison with Vapor Phase Reaction," *Ind. Eng. Chem. Process. Des. Dev.*, **23,** 11 (1984).

Schwartz, J. G., E. Weger, and M. P. Dudukovic, "A New Tracer Method for Determination of Liquid-Solid Contacting Efficiency in Trickle-Bed Reactors," *AIChE J.*, **22,** 894 (1976).

Somers, A., Y. T. Shah, and J. Paraskos, "Kinetics of Diolefin Hydrogenation in a Trickle-Bed Reactor," *Chem. Eng. Sci.*, **31,** 759 (1976).

Stegmuller, R., A. Cukierman, and N. O. Lemcoff, "Selectivity of Complex Reactions in Trickle-Bed Reactors," *Chem. Eng. Commun.*, **41,** 291 (1986).

Tan, C. S., and J. M. Smith, "Catalyst Particle Effectiveness with Unsymmetrical Boundary Conditions," *Chem. Eng. Sci.*, **35,** 1601 (1980).

Teramoto, M., T. Nagayasu, T. Matsui, K. Hashimoto, and S. Nagata, "Selectivity of Consecutive Gas-Liquid Reactions," *J. Chem. Eng. Japan*, **2,** 186 (1969).

van de Vusse, J. G., "Consecutive Reactions in Heterogeneous Systems. I: The Effect of Mass Transfer on Selectivity," *Chem. Eng. Sci.*, **21,** 631 (1966a).

———, "Consecutive Reactions in Heterogeneous Systems. II: Influence of Order of Reaction Rates on Selectivity," *Chem. Eng. Sci.*, **21,** 645 (1966b).

Wei, J., "Intraparticle Diffusion Effects in Complex Systems of First-Order Reactions," *J. Catal.*, **1,** 526 (1962).

Wheeler, A., "Reaction Rates and Selectivity in Catalyst Pores," *Catalysis*, 2nd. ed., P. H. Emmett, ed., Reinhold, New York (1955).

White, D. E., and M. Litt, "Diffusion-Limited Heterogeneous Catalytic Reactions on a Rotating Disk. II: Hydrogenation of Phenylacetylene over Palladium," *Ind. Eng. Chem. Fundam.*, **14,** 83 (1975).

Wisniak, T., and R. Simon, "Hydrogenation of Glucose, Fructose, and Their Mixtures," *Ind. Eng. Chem. Process. Des. Dev.*, **18**, 50 (1979).
Yentekakis, I. V., and C. G. Vayenas, "Effectiveness Factors for Reactions Between Volatile and Non-Volatile Components in Partially Wetted Catalysts," *Chem. Eng. Sci.*, **42**, 1323 (1987).

Manuscript received Aug. 11, 1987, and revision received Jan. 26, 1988.

See NAPS document no. 04580 for 52 pages of supplementary material. Order from NAPS c/o Microfiche Publications, P.O. Box 3513, Grand Central Station, New York, NY 10163. Remit in advance in U.S. funds only $7.75 for photocopies or $4.00 for microfiche. Outside the U.S. and Canada, add postage of $4.50 for the first 20 pages and $1.00 for each of 10 pages of material thereafter, $1.50 for microfiche postage.